Materials Letters 135 (2014) 55–58

Contents lists available at ScienceDirect

Materials Letters

journal homepage: www.elsevier.com/locate/matlet

$ZnMn_2O_4$ mesocrystals for lithium-ion batteries with high rate capacity and cycle stability

Rencheng Jin*, Quanwu Wen, Lixia Yang, Guihua Li

School of Chemistry & Materials Science, Ludong University, Yantai 264025, PR China

ARTICLE INFO

Article history:
Received 2 June 2014
Accepted 20 July 2014
Available online 1 August 2014

Keywords:
Crystal growth
Energy storage and conversion
Nanocrystalline materials

ABSTRACT

$ZnMn_2O_4$ mesocrystals have been fabricated through an effective, inexpensive molten salt method. Scanning electron microscopy and transmission electron microscopy observations confirm that the as-prepared $ZnMn_2O_4$ nanoparticles (20–50 nm in diameter) uniformly aggregate into mesocrystals. Electrochemical investigation shows that the $ZnMn_2O_4$ mesocrystals exhibit excellent cycling performance (608 mAh g^{-1} at 100 mA g^{-1} up to 100 cycles) and high rate capability. The results suggest that $ZnMn_2O_4$ mesocrystal is a promising candidate for practical application as lithium ion battery anode material.

1. Introduction

Nowadays, nanomaterials with highly ordered superstructures have attracted considerable attention and the fabrication of such structures is still a great challenge. Mesocrystal, firstly proposed by Cölfen et al. [1,2], represents a new kind of superstructures consisting of oriented aggregated primary crystallites and behaves like single crystal. Compared with the primary crystallites, mesocrystals present both high crystallinity approaching single-crystalline and high specific surface area, which possess potentially exciting applications in many fields. Therefore, various inorganic mesocrystalline architectures have been fabricated to improve their properties. For example, TiO_2 and Fe_2O_3 mesocrystals with high charge–discharge capacity and cycling stability for anode materials in lithium ion cells have been fabricated [3,4]. CuO mesocrystals have been synthesized through an electrochemical method, which exhibit good lithium storage properties [5].

$ZnMn_2O_4$, a transition metal oxide, has been considered as a potential high-performance anode material because of its low cost, environment friendliness and much lower operating voltage in comparison with the Co or Fe based oxides [6,7]. However, this material presents large volume change during charging and discharging processes and severe electron conduction restriction during the electrochemical reaction, which limits its application in lithium ion batteries (LIBs) [8]. Therefore, improving the discharge capacity and cycling stability becomes a hot topic for $ZnMn_2O_4$. The previous literatures reported that metal oxides with nanostructure had the advantages of short path length for Li^+ transport and high surface-to-volume ratio [9,10]. For example, one-dimensional $ZnMn_2O_4$ nanowires, nanorods, nanofibers, and nanowebs have been fabricated, which reveal high discharge capacity due to the enhanced kinetics of the nanowire and the higher surface area of nanofibers [11–13]. Three dimensional flower-like $ZnMn_2O_4$ superstructures and hollow microspheres exhibiting the high specific discharge capacity and cycling stability have been prepared [8,14,15]. However, the synthesis of these nanostructures is complicated and some surfactants are needed. Thus, a facile method for the preparation of $ZnMn_2O_4$ with well-defined composition and morphology is needed. Herein, two dimensional $ZnMn_2O_4$ mesocrystals were successfully synthesized by using a facile molten salt route. When evaluated as an anode material for LIBs, the as-synthesized $ZnMn_2O_4$ exhibited superior electrochemical properties including good rate capability and excellent cycling performance.

2. Experimental section

Materials preparation: In the typical procedure, 1 mmol of $Zn(Ac)_2$, 2 mmol of $Mn(Ac)_2$ and 10 g of mixed salts (NaCl/KCl with the mass ratio of 5/5) were added in the agate mortar. After grinding for about 30 min, the mixture was transformed into an alumina crucible and maintained at 650 °C for 6 h. Then the alumina crucible was cooled naturally to room temperature and washed with distilled water and absolute ethanol for several times. The obtained clayblank products were dried at 80 °C overnight.

Materials characterization: The phase and composition of the prepared products were characterized by a D/max-2550 PC X-ray

---

* Corresponding author.
E-mail address: jinrc427@126.com (R. Jin).

http://dx.doi.org/10.1016/j.matlet.2014.07.132
0167-577X/© 2014 Elsevier B.V. All rights reserved.

diffractometer (XRD, Rigaku, Cu-Kα radiation). The structure and morphology of the product were detected by a FEI Quanta 200F field emission scanning electron microscopy (FESEM) and FEI Tecnai G2 S-Twin transmission electron microscopy (TEM).

Electrochemical measurement: Electrochemical performance of the as-synthesized active materials was performed on a NEWWAY battery test system using coin-type cells (CR 2025). Working electrodes were prepared by mixing the obtained products (70 wt%) with acetylene black (15 wt%) and polyvinylidene fluoride (PVDF, 15 wt%) in N-methyl-2-pyrrolidone (NMP). After stirring the mixture for 6 h, the homogenous slurry was coated on the copper foil, and then dried in the vacuum at 100 °C overnight. The electrolyte was consisted of a solution of 1 mol L^{-1} $LiPF_6$ in a mixture of ethylene carbonate (EC)–diethylene carbonate (DEC) (1:1 vol%). The metallic lithium and the Celgard 2400 film were used as the counter/reference electrode and the separator, respectively. The cells were assembled in an argon-filled glove box. The charge–discharge cycles of the cells were evaluated between 0.01 and 3 V at different current densities (100 mA g^{-1}, 200 mA g^{-1}, 500 mA g^{-1}, 1000 mA g^{-1}).

3. Results and discussion

The X-ray diffraction pattern of the obtained products is shown in Fig. 1a. All diffraction peaks can be readily assigned to the tetragonal $ZnMn_2O_4$ (JCPDS card no. 24-1133). The weak and wide diffraction peaks indicate the poor crystallinity of the as prepared $ZnMn_2O_4$. Scanning electron microscopy (SEM) and transmission electron microscopy (TEM) are used to reveal the morphology and microstructure of the as prepared $ZnMn_2O_4$. Fig. 1b and c shows that $ZnMn_2O_4$ consists of numerous nanosheets with the thickness of 50–130 nm. The enlarged SEM image (Fig. 1c) presents that the nanosheets are composed of a large amount of nanoparticles with the diameter of 20–50 nm. The TEM image (Fig. 1d) further proves that the nanosheets are assembled by nanoparticles. Fig. 1e reveals a representative HRTEM image of the corner of nanosheet. The interplanar spacing is about 0.49 nm, corresponding to the (101) plane of $ZnMn_2O_4$. The selected-area electron diffraction (SAED) of a single nanosheet in Fig. 1f displays a typical single crystalline spot. Meanwhile, the misorientations deviating from perfect alignment between nanocrystallites can be reflected clearly by the elongated diffraction spots in the SAED pattern. According to the XRD, SEM, HRTEM and SAED results, one can conclude that the nanoparticles can aggregate together to form the $ZnMn_2O_4$ mesocrystals.

The electrochemical performance of the $ZnMn_2O_4$ nanosheets is evaluated by galvanostatic charge–discharge cycling and electrochemical impedance spectroscopy. Fig. 2a displays a charge–discharge curve for the first, second and fifth cycles of the $ZnMn_2O_4$ electrode at a current density of 100 mA g^{-1}. The first discharge capacity is 1309.5 mAh g^{-1}, which is higher than those of the reported $ZnMn_2O_4$ nanocrystals [16] (1032 mAh g^{-1}) and nanoflakes (1088 mAh g^{-1}) [17]. The irreversible loss between the first charge and discharge cycles is about 364 mAh g^{-1}. The initial coulombic efficiency is 70.8% (Fig. 2b), which is higher than those of the loaf-like (61.8%) and flower-like $ZnMn_2O_4$ (56.5%) [8,12]. This may be attributed to the mesostructure of $ZnMn_2O_4$, reducing the capacity from the irreversible reactions on the surface. Fig. 2b presents the discharge/charge cyclic properties of the $ZnMn_2O_4$ nanosheets in the voltage range of 0.01–3.0 V at current densities of 100 mA g^{-1}. In the first 10 cycles, the cycling property of the $ZnMn_2O_4$ electrodes was in the transition phase from an unstable to a stable condition. After 100 cycles, the capacity still retains 608 mAh g^{-1}, demonstrating the long-term cycling stability and enhanced reversible capacity of these electrodes. Besides the first cycle, the coulombic efficiency of $ZnMn_2O_4$ electrodes is higher than 97%. This high coulombic efficiency further confirms the high electrochemical stability of the products. To evaluate the rate capacity, the $ZnMn_2O_4$ electrode is cycled at different current densities (100–1000 mA g^{-1}). The charge capacities of 678, 575,

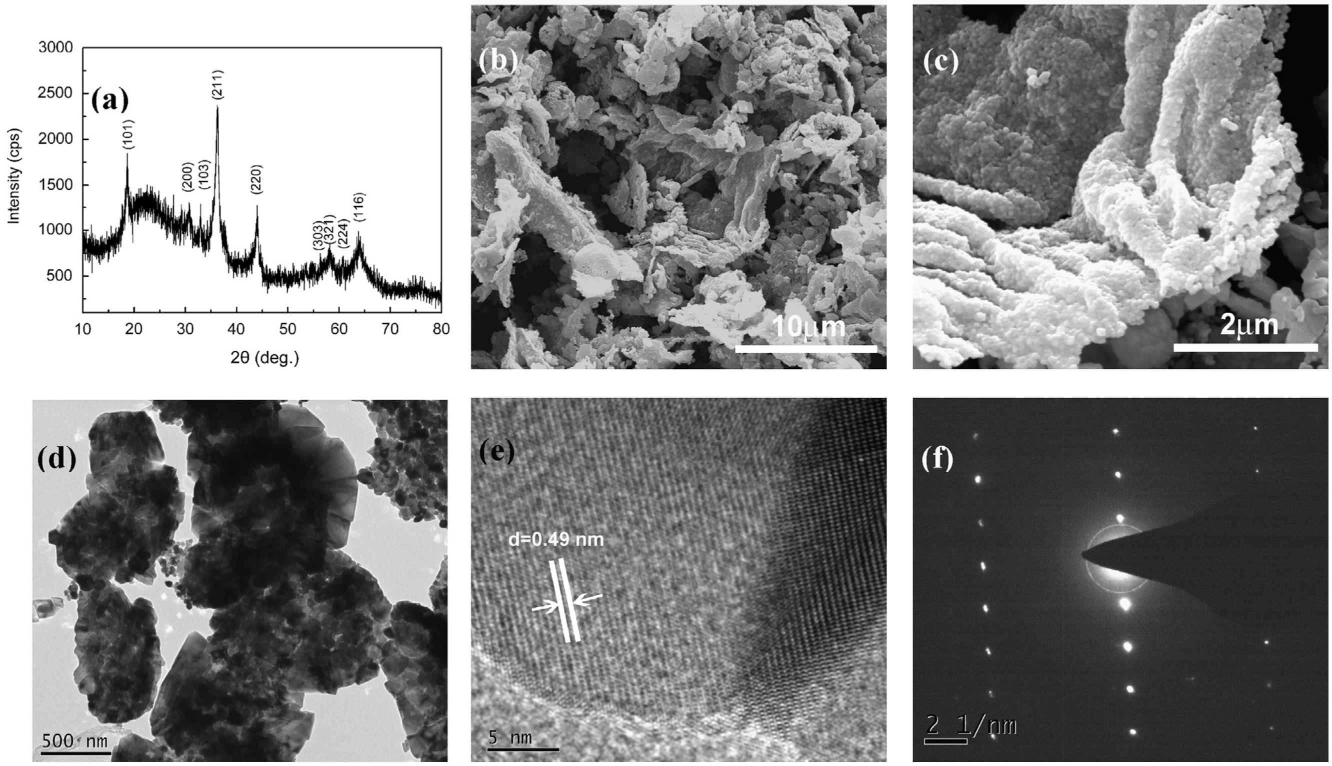

Fig. 1. Characterization of $ZnMn_2O_4$ mesocrystals prepared at 650 °C for 6 h (a) XRD pattern, (a) low magnification FESEM image, (c) high magnification FESEM image, (d) TEM image, (e) HRTEM image, (f) SAED pattern.